A numerical study of residual circulation induced by asymmetric tidal mixing in tidally dominated estuaries

Peng Cheng,[1,2] Arnoldo Valle-Levinson,[1] and Huib E. de Swart[3]

Received 21 January 2010; revised 11 October 2010; accepted 16 November 2010; published 27 January 2011.

[1] Residual currents induced by asymmetric tidal mixing (ATM) were examined using a series of idealized numerical experiments for weakly stratified, partially mixed, and highly stratified narrow estuaries that neglected lateral variations of bathymetry and the effects of Earth's rotation. The Eulerian residual currents were decomposed into four components, i.e., river-induced, density-driven, nonlinearities-induced, and ATM-induced flows such that the longitudinal distribution and strength of each component can be depicted and evaluated. In weakly stratified estuaries, ATM-induced flow has a two-layer structure similar to that of density-driven flow. It reinforces the estuarine exchange flow. In partially mixed and highly stratified estuaries, the ATM-induced flow tends to have a three-layer structure with landward flows near the surface and the bottom and seaward flow in the middle of the water column. It appears to act against the estuarine exchange flow in parts of the water column. The relative importance of ATM-induced flow to estuarine residual currents varies in different types of estuaries. Compared to the density-driven flow, the relative importance of ATM-induced flow decreases as stratification increases. In the central regime of the estuary, the strength of the ATM-induced flow is greater than that of density-driven flow under weak stratification and tends to be smaller under strong stratification.

Citation: Cheng, P., A. Valle-Levinson, and H. E. de Swart (2011), A numerical study of residual circulation induced by asymmetric tidal mixing in tidally dominated estuaries, *J. Geophys. Res.*, *116*, C01017, doi:10.1029/2010JC006137.

1. Introduction

[2] The conventional view on the dynamics of residual estuarine circulation has assumed constant vertical mixing that neglects temporal and spatial variations [*Pritchard*, 1956; *Hansen and Rattray*, 1966; *Chatwin*, 1976; *Officer*, 1976; *McCarthy*, 1993; *MacCready*, 2004; *Talke et al.*, 2009]. This simplified treatment of turbulent mixing is convenient to obtain analytical solutions and is able to describe the essential features of density-driven flow, i.e., the vertical two-layer structure. Recent studies have acknowledged that turbulent mixing varies and is asymmetric during a tidal cycle, typically stronger during flood than ebb tides. This asymmetric tidal mixing (hereafter ATM) is usually known as internal tidal asymmetry [*Jay and Smith*, 1990]. In estuaries, strain-induced periodic stratification (SIPS or tidal straining, *Simpson et al.* [1990]) is a dominant mechanism creating tidal asymmetry because of the existence of a longitudinal density gradient. During ebb tides, tidal currents stratify the water column through the straining of the density field and create a vertically sheared velocity profile. During flood tides, this straining is reversed and the bottom water column tends to be destratified, intensifying currents near the bottom. Thus, the asymmetric mixing and velocity profiles can lead to a residual flow with the same structure as the density-driven circulation, namely seaward flow near the surface and landward flow near the bottom [*Jay and Musiak*, 1996; *Stacey et al.*, 2001].

[3] Using a one-dimensional numerical model with a two-equation turbulent closure, *Stacey et al.* [2008] simulated tidal waves with periodic stratification imposed at a particular phase of each tidal cycle. Their results demonstrated that the residual flow generated by typical ATM, i.e., turbulent mixing being stronger during flood than ebb tides, had the same vertical structure and magnitude as estuarine gravitational circulation. They also found that the magnitude of the resulting residual flow was strongly dependent upon the timing of stratification beginning within the tidal cycle and they pointed out that stratification induced during the flood tide (e.g., reversed ATM) leads to a very different residual flow structure than stratification created during the ebb tide (e.g., typical ATM). *Burchard and Hetland* [2010] derived mathematical definitions of ATM-induced and gravitational circulation for periodically stratified tidal estuaries and quantified the relative importance of the two processes in creating estuarine residual flow using a one-dimensional numerical model. They found that for situations without

[1]Department of Civil and Coastal Engineering, University of Florida, Gainesville, Florida, USA.
[2]Now at Large Lakes Observatory, University of Minnesota, Duluth, Minnesota, USA.
[3]Institute for Marine and Atmospheric Research Utrecht, Utrecht University, Utrecht, Netherlands.

0148-0227/11/2010JC006137

wind straining and residual runoff, ATM contributes two thirds and gravitational circulation contributes one third to the estuarine circulation.

[4] With a two-dimensional analytical model, *Cheng et al.* [2010] examined the residual currents induced by ATM in weakly stratified narrow estuaries, which can be treated as weakly nonlinear systems. The results confirmed the vertical structure of the ATM-induced flow revealed by previous studies. Moreover, the 2-D model showed that the along-estuary distribution of ATM-induced flow was determined by tidal current amplitude, asymmetries in tidal mixing and tidal mean mixing. In addition, both the magnitude and the vertical structure of ATM-induced flow responded to asymmetries in tidal mixing. Larger asymmetries in tidal mixing produced stronger residual currents and reversed tidal asymmetry generated a vertical profile of along-estuary flow that was opposite to that produced by typical tidal asymmetry.

[5] Although the analytical model of *Cheng et al.* [2010] revealed some essential features of ATM-induced flows, the results were limited to weakly stratified estuaries. Moreover, the simplified treatment of turbulent mixing, such as an artificially prescribed eddy viscosity, jeopardizes the generality of the analytical model. In order to overcome limitations of that analytical model, in this study a series of idealized numerical experiments were conducted using a three-dimensional primitive equations numerical model with a two-equation turbulence closure. The main objective of this study is to examine ATM-induced flows in estuaries with a wide range of stratification conditions. Three types of estuaries: weakly stratified, partially mixed and highly stratified estuaries are explored. Inspired by the analytical model, a method was developed to calculate the four components of the residual currents (i.e., river-induced, density-driven, nonlinearities-induced, and ATM-induced flows) from the numerical model results. This allows examination of the spatial patterns of the four components, and evaluation of the relative contribution of each component to estuarine exchange flow.

[6] Lateral circulation has been recognized as an important contributor to estuarine exchange flow [*Lerczak and Geyer*, 2004; *Huijts et al.*, 2009; *Cheng and Valle-Levinson*, 2009]. Lateral processes can lead to estuarine stratification on either phase of tides generating asymmetric tidal mixing [*Lacy et al.*, 2003; *Fram et al.*, 2007; *Stacey et al.* 2008] and can redistribute along-estuary momentum to counteract the effect of tidal asymmetry on the residual circulation [*Scully et al.*, 2009]. However, in this study, we minimize lateral processes and focus our attention specifically on narrow estuaries where lateral variations of bathymetry and the effects of Earth's rotation are negligible. Our goal here is not to provide a realistic simulation for a particular estuary, but rather to gain insights into basic characteristics of ATM-induced residual currents. The role of lateral processes on tidal asymmetry must await future studies.

[7] The remainder of this paper is organized as follows. Section 2 describes the numerical model configuration and presents the method to decompose residual currents. Section 3 depicts along-estuary patterns of river-induced, density-driven, nonlinearities-induced, and ATM-induced flows in weakly stratified, partially mixed and highly stratified estuaries. Section 4 addresses four issues relevant to tidal asymmetry: (1) measurement of asymmetries in tidal mixing; (2) causes of the vertical structure of the ATM-induced flow; (3) spatial patterns of turbulent mixing in the central regime of the estuaries; and (4) strength of ATM-induced flow as well as its contribution to residual estuarine circulation. Finally, conclusions are presented in section 5.

2. Numerical Model and Methods

2.1. Numerical Model Configuration

[8] The Regional Ocean Modeling System (ROMS) was used to carry out idealized experiments. The model is a free surface, hydrostatic, primitive equations ocean model that uses stretched, terrain-following vertical coordinates and orthogonal curvilinear horizontal coordinates on an Arakawa C grid [*Haidvogel et al.*, 2000]. The model configuration is similar to that given by *Cheng et al.* [2010]. The model domain is designed as an estuary shelf system (Figure 1). The part of the domain corresponding to the estuary is straight, 300 km long and has no along-channel bottom slope. The cross-channel section has a rectangular shape with a depth of 10 m and a width of 600 m. Freshwater discharge is specified at the head of the estuary and a semidiurnal tide (S_2) is imposed at the eastern boundary. The river discharge and tidal amplitude are adjustable. The inflowing river water is prescribed to have zero salinity and a temperature of 15°C, identical to the background temperature set throughout the entire domain. The continental shelf is 80 km wide and has a fixed cross-shelf slope of 0.05%. The salinity of the coastal ocean is 35 psu and a southward weak flow (0.03 m s^{-1}) is specified on the shelf to suppress the bulge of freshwater at the estuary mouth. The coastal ocean is included in the domain to avoid specifying boundary conditions at the estuary mouth, which are usually difficult to establish. The two-equation turbulence closure k-ω is used to calculate vertical mixing.

[9] The model grid is 200 (along-channel, x-direction) by 80 (cross-channel, y-direction) by 40 (vertical, z-direction) cells. The river has 160 grid cells along the channel and 3 grid cells across the channel. The small number of cross-channel cells is designed to minimize effects of lateral processes. The along-channel grid size (Δx) increases exponentially from the estuary's mouth (~50 m) to its head (~12 km), providing a highly resolved region near the estuary's mouth. The cross-channel grid in the estuary is uniformly distributed and the vertical layers are uniformly discretized. The model runs, from rest, for 70 d until reaching steady state. The results of the last day of simulation are used for analysis.

2.2. Decomposition of Residual Currents

[10] Residual currents can be readily computed by taking the tidal average of the numerical model output. However, these residual currents contain several components induced by different mechanisms such as river discharge, horizontal density gradients and tidal processes. Accordingly, it is necessary to separate those components in order to characterize the residual flow induced by asymmetric tidal mixing. The method presented here follows the same logic of the analytical models of *Ianniello* [1977], *McCarthy* [1993] and

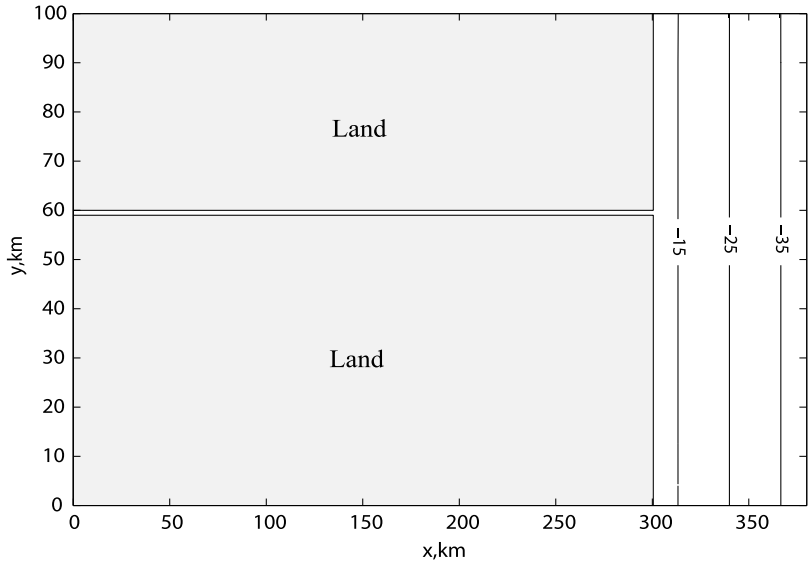

Figure 1. Domain of numerical model. Contours denote water depth on the shelf.

Cheng et al. [2010]. On the basis of the simple geometry of the modeled estuary channel, the width-averaged governing equations for along-channel momentum and continuity are

$$\frac{\partial u}{\partial t}+u\frac{\partial u}{\partial x}+w\frac{\partial u}{\partial z}=-g\frac{\partial \eta}{\partial x}-\frac{g}{\rho_0}\int_z^{\eta}\frac{\partial \rho}{\partial x}dz+\frac{\partial}{\partial z}\left(K_m\frac{\partial u}{\partial z}\right), \quad (1a)$$

$$\frac{\partial \eta}{\partial t}+\frac{\partial}{\partial x}\left(\int_{-H}^{0}udz\right)+\frac{\partial}{\partial x}\left(u|_{z=0}\eta\right)=0. \quad (1b)$$

Here, u and w are the longitudinal (x-direction) and vertical (z-direction) velocity components, respectively, g is the gravitational acceleration, η is the free surface elevation, H is the mean water depth, ρ is water density, ρ_0 is a reference water density, and K_m is the vertical eddy viscosity. All these variables are averaged across the estuary channel. According to *Ianniello* [1977], equation (1b) is an approximation assuming small η relative to H, obtained by replacing the depth integral of u from $-H$ to η by the integral from $-H$ to 0 plus the first term of the series expansion of the integral from 0 to η, such that the longitudinal water flux is decomposed into two terms representing Eulerian transport (the second term in equation (1b)) and net water transport induced by the tidal wave (or Stokes transport, the third term in equation (1b)), respectively. The residual currents studied in this work are Eulerian, which are obtained from time-averaging of equations (1a) and (1b) over a tidal cycle:

$$\overline{u\frac{\partial u}{\partial x}}+\overline{w\frac{\partial u}{\partial z}}=-g\frac{\partial \overline{\eta}}{\partial x}-\frac{g}{\rho_0}\int_z^{0}\frac{\partial \overline{\rho}}{\partial x}dz+\frac{\partial}{\partial z}\left(\overline{K_m\frac{\partial u}{\partial z}}\right), \quad (2a)$$

$$\int_{-H}^{0}\overline{u}dz+\overline{u|_{z=0}\eta}=R. \quad (2b)$$

In these expressions, the overbar denotes tidal averages, R is the river discharge per unit width (in $m^2\ s^{-1}$). K_m and u are separated into tidal mean and tidal variation components, i.e., $K_m=\overline{K_m}+K_m'$, $u=\overline{u}+u'$. Here, $\overline{K_m}$ and $\overline{u}$ represent the tidal mean, while K_m' and u' represent the tidal fluctuation parts. The residual currents ($\overline{u}$) are considered to have four components: (1) the river-induced flow ($\overline{u_R}$); (2) the density-driven flow ($\overline{u_D}$); (3) the nonlinearities-induced flow ($\overline{u_N}$); and (4) the flow induced by asymmetric tidal mixing ($\overline{u_A}$). Thus, $\overline{u}$ and the corresponding residual free surface elevation $\overline{\eta}$ can be written as

$$\overline{u}=\overline{u_R}+\overline{u_D}+\overline{u_N}+\overline{u_A}, \quad (3a)$$

$$\overline{\eta}=\overline{\eta_R}+\overline{\eta_D}+\overline{\eta_N}+\overline{\eta_A}. \quad (3b)$$

[11] Substituting equations (3a) and (3b) into (2a) and (2b) yields a set of four momentum and four continuity equations corresponding to the four components of the residual currents:

$$0=-g\frac{\partial \overline{\eta_R}}{\partial x}+\frac{\partial}{\partial z}\left(\overline{K_m}\frac{\partial \overline{u_R}}{\partial z}\right), \quad (4a)$$

$$\int_{-H}^{0}\overline{u_R}dz=R, \quad (4b)$$

for river-induced flow,

$$0=-g\frac{\partial \overline{\eta_D}}{\partial x}-\frac{g}{\rho_0}\int_z^{0}\frac{\partial \overline{\rho}}{\partial x}dz'+\frac{\partial}{\partial z}\left(\overline{K_m}\frac{\partial \overline{u_D}}{\partial z}\right), \quad (5a)$$

$$\int_{-H}^{0}\overline{u_D}dz=0, \quad (5b)$$

for density-driven flow,

$$\overline{u\frac{\partial u}{\partial x}} + \overline{w\frac{\partial u}{\partial z}} = -g\frac{\partial \overline{\eta_N}}{\partial x} + \frac{\partial}{\partial z}\left(\overline{K_m}\frac{\partial \overline{u_N}}{\partial z}\right), \tag{6a}$$

$$\int_{-H}^{0} \overline{u_N}dz + \overline{u|_{z=0}\eta} = 0, \tag{6b}$$

for nonlinearities-induced flow, and

$$0 = -g\frac{\partial \overline{\eta_A}}{\partial x} + \frac{\partial}{\partial z}\left(\overline{K_m}\frac{\partial \overline{u_A}}{\partial z}\right) + \frac{\partial}{\partial z}\left(\overline{K_m'\frac{\partial u'}{\partial z}}\right), \tag{7a}$$

$$\int_{-H}^{0} \overline{u_A}dz = 0, \tag{7b}$$

for ATM-induced flow.

[12] The boundary conditions used to solve the four sets of equations (equations (4a)–(7b)) are no slip at the bottom and no shear at the surface. The solutions are presented in the Appendix. Taking advantage of the numerical model output, the variables: u, w, R, $\overline{\rho}$, $\overline{u}$, $\overline{K_m}$, u' and K_m' in the equations are known, such that the four components of the residual flows can be calculated numerically. Note that in case of a tidally dominated estuary in which residual currents are weak compared to tidal currents, $\overline{u_N}$ can be considered as a flow (e.g., tidal-nonlinearities-induced flow) that is induced by advection of tidal momentum by the tidal flow. In that case, the different flow components are uniquely related to different forcing agents. If the system is not tide-dominated, then the flow component $\overline{u_N}$ has a slightly different interpretation, as it is also affected by advection of residual momentum by residual flow.

3. Results

[13] Stratification in an estuary is mainly determined by the competition between buoyancy input from river discharge and vertical turbulent mixing of which tide is a dominant mixing agent. A series of numerical experiments were carried out for a number of different values of tidal amplitude at the eastern boundary and river discharge in order to simulate different types of estuaries. Three experiments were selected to represent weakly stratified, partially mixed and highly stratified estuaries, respectively. These types of estuaries loosely follow the classification of coastal plain estuaries [*Pritchard*, 1955; *Cameron and Pritchard*, 1963]. Because well-mixed estuaries have no stratification-induced asymmetric tidal mixing, a weakly stratified estuary is taken as an approximately well-mixed estuary with weak influences from vertical stratification. The highly stratified estuary is considered as an estuary with a stable two-layer structure (separated by a sharp halocline) throughout a tidal cycle, while the partially mixed estuary is stratified over a tidal cycle but has no permanent two-layer structure. Even though these criteria for estuary classification are not strict, the three numerical experiments presented below show, in a general sense, the influences of stratification on ATM-induced flow.

[14] The four components of residual currents were calculated for the three types of estuaries using the above method. Because water surface fluctuates around mean water level, the integration of the water column is taken from the bottom to the lowest water level (e.g., $-\eta$) during a tidal cycle. The influence of water level fluctuations on Eulerian residual currents is neglected here. The validation of this assumption needs to be addressed in future studies. Because of the simplified geometry of the river channel (rectangular transverse section) and model setup, the lateral variations of residual currents are minimized in the results. The objective of this section is to present the along-estuary patterns of the four residual flow components with an emphasis on the ATM-induced flow.

3.1. Weakly Stratified Estuary

[15] In the numerical experiment of the weakly stratified estuary, the tidal amplitude at the eastern open boundary is 1.5 m and the section-averaged freshwater velocity imposed at the river head is 0.01 m s^{-1}. The longitudinal distribution of the tidally averaged salinity shows slightly tilted isohalines (Figure 2a) indicating the influence of weak stratification. The tidally and depth averaged salinity (Figure 2d) exhibits the general form of the hyperbolic tangent function expected in coastal plain estuaries [*Pritchard*, 1952; *Hansen and Rattray*, 1966]. Salinity increases downstream and gradually reaches the terminal value of the ocean. The maximum horizontal salinity gradient occurs around x = 286 km (Figure 2g). Near the estuary mouth (286– 300 km), the horizontal salinity gradient decreases and the curvature of the salinity curve is negative. This is attributed to the strong tidal dispersion near the estuary mouth [*McCarthy*, 1993; *MacCready*, 2004]. According to the salinity distribution, the central regime of the estuary is defined at 262–286 km. The tidally and depth averaged eddy viscosity is notably reduced (Figure 2j) in the central regime, the region with largest along-estuary density gradients. This longitudinal distribution of the eddy viscosity challenges the assumption used in some previous studies that the eddy viscosity is constant throughout the entire estuary. The reduction of turbulent mixing in the central regime results in peculiar characteristics of the residual currents, as illustrated later.

[16] Longitudinal patterns of residual currents are shown in Figure 3. The river-induced flow ($\overline{u_R}$) is reminiscent of an open channel flow. In the estuarine region, the magnitude and the shear of the flow markedly increase. However, the water flux is still conserved because the residual water surface level is reduced. The density-driven flow ($\overline{u_D}$) shows a typical two-layer structure with seaward flow near the surface and landward flow near the bottom. The magnitude of $\overline{u_D}$ is the greatest in the central regime of the estuary because of the large horizontal salinity gradient and the reduced turbulent mixing. The strength of the nonlinearities-induced flow ($\overline{u_N}$) increases toward the estuary mouth, following the trend of the Stokes drift. The general pattern of $\overline{u_N}$ is consistent with that predicted by analytical models [*Ianniello*, 1977, 1981; *McCarthy*, 1993]. Reduced turbulent mixing in the central regime enhances shear and, thus, increases current amplitudes near the surface. The ATM-induced flow ($\overline{u_A}$) has a two-layer structure that is similar to the density-driven flow

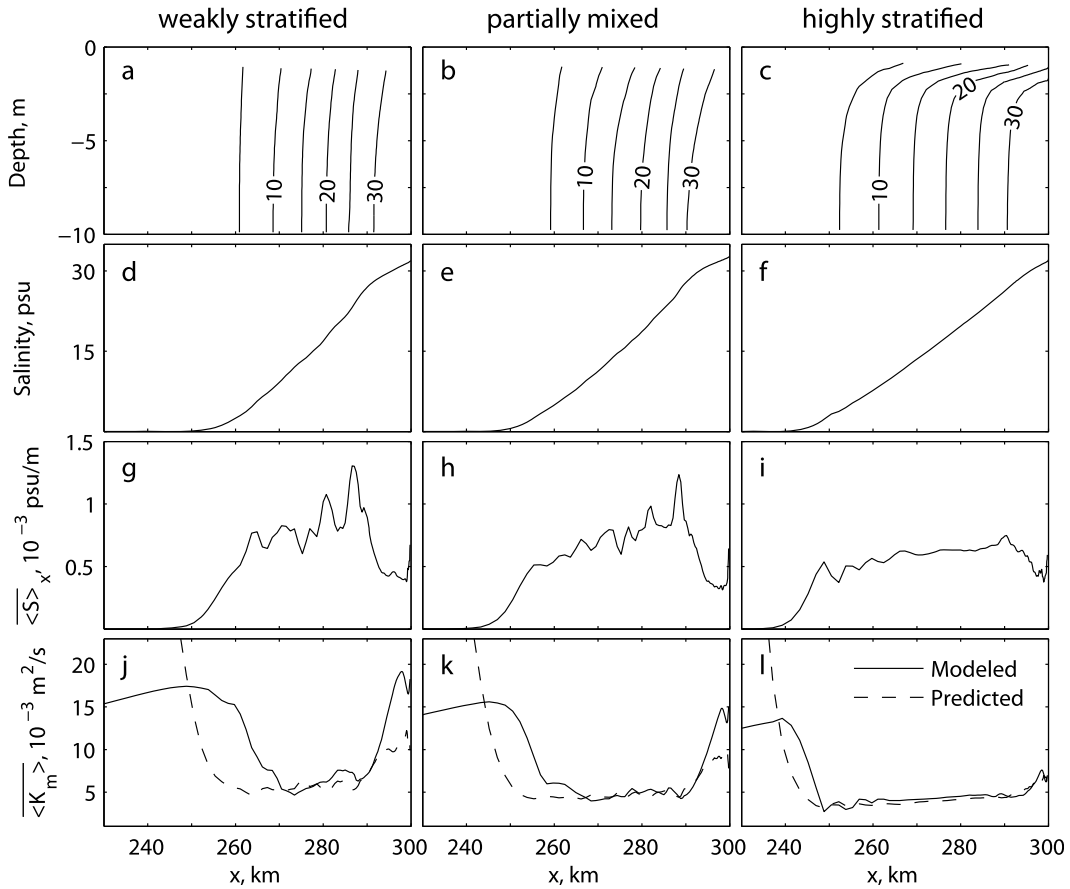

Figure 2. Along-estuary distributions of tidally averaged salinity and eddy viscosity. (a-c) The salinity field; (d-f) the depth-mean salinity; (g-i) the along-estuary gradient of depth-mean salinity; (j-l) the depth-mean eddy viscosity. In Figures 2j–2l, solid lines are model results, while dashed lines are predicted by equation (9).

but with maximum velocities near the estuary mouth. The longitudinal distribution of $\overline{u_A}$ generally agrees with that predicted by the analytical model of *Cheng et al.* [2010] for a flow induced by typical asymmetric tidal mixing. The four components of residual currents, added together, were compared to the total residual flow ($\overline{u}$) obtained by directly taking the tidal average of the numerical output. The two total residual flows agree with each other very well, indicating the intrinsic coherence. The total residual flow shows a pattern of exchange flow with much stronger seaward currents in the upper layer. The imbalance of water flux generates a net outflow which is compensated by the inward Stokes return flow.

3.2. Partially Mixed Estuary

[17] In the numerical experiment of the partially mixed estuary, the tidal amplitude at the eastern open boundary is 1.2 m and the section-averaged fresh water velocity imposed at the river head is 0.01 m s^{-1}. The tidally averaged salinity field and eddy viscosity (Figures 2b, 2e, 2h, and 2k) are similar to those of the weakly stratified estuary. The length of estuary (distance of salt intrusion discerned from the depth-mean salinity) is longer than that of the weakly stratified estuary because of weaker turbulent mixing. The maximum along-channel salinity gradient is located around x = 288 km and the central regime of the estuary is taken between x = 258 and 288 km. If the distance from the maximum along-channel salinity gradient to the estuary mouth is used as a measurement of the tidal dispersion length, the partially mixed estuary has a weaker tidal dispersion than the weakly stratified estuary, owing to the smaller tidal amplitude.

[18] The longitudinal patterns of $\overline{u_R}$, $\overline{u_D}$, and $\overline{u_N}$ are similar to those of the weakly stratified estuary (Figure 4). The residual flows tend to be highly sheared and intensified, particularly near the surface because of increased stratification. $\overline{u_A}$ shows notable changes in the longitudinal pattern. In the outer regime of the estuary (from x = 288 km to the estuary mouth), $\overline{u_A}$ has the typical two-layer structure similar to that of density-driven flow. In the central regime of the estuary, $\overline{u_A}$ shows a three-layer structure with landward flows near the surface and bottom and seaward flow in the middle water column. Comparing $\overline{u_D}$ to $\overline{u_A}$, the latter tends to compensate the seaward flow near the surface and the landward flow in the middle water column. It appears that tidal asymmetry plays a comparatively complicated role in the creation of estuarine exchange flow. The causes of the three-layer structure of $\overline{u_A}$ are explored in section 4.2.

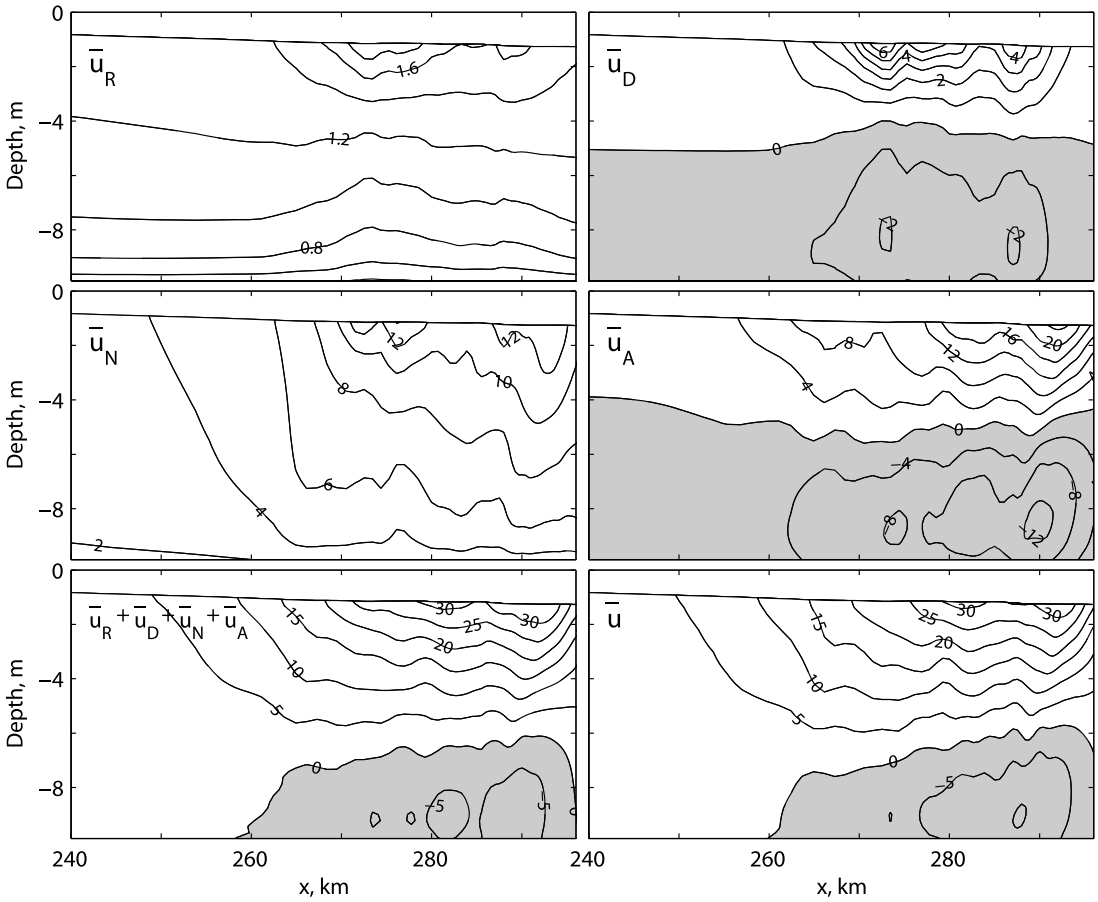

Figure 3. Along-estuary patterns of river-induced ($\overline{u_R}$), density-driven ($\overline{u_D}$), nonlinearities-induced ($\overline{u_N}$), asymmetric tidal mixing (ATM)–induced ($\overline{u_A}$), and total Eulerian ($\overline{u}$) residual flows for the weakly stratified estuary. The first four residual flows are calculated using the decomposition method (e.g., equations (A1)–(A8)) while the total residual flow is obtained by tidally averaging the modeled current velocity. The units of the residual flows are cm s^{-1}. Negative values (shaded) denote landward flow.

3.3. Highly Stratified Estuary

[19] In the numerical experiment of the highly stratified estuary, the tidal amplitude at the eastern open boundary is 1.0 m and the section-averaged fresh water velocity imposed at the river head is 0.05 m s^{-1}. The relatively large tidal amplitude (1 m) applied in this case may be unrealistic for highly stratified estuaries where tides tend to be of low amplitude (<0.5 m). The purpose of this choice, however, is to simulate an appreciable influence from tides. The tidally averaged salinity field shows a sharp halocline located around the depth of 2.5 m indicating a highly stratified estuary (Figure 2c). The thickness of the lower layer underneath the halocline includes a great portion of the water column because of the relatively strong tide. The depth-mean salinity increases approximately linearly in the central regime of the estuary (Figure 2f) so that the assumption of constant along-channel salinity gradient is valid in the central regime of the highly stratified estuary (Figure 2i). The maximum along-channel salinity gradient is found at around $x = 292$ km and the central regime of the estuary can be defined between $x = 250$ and 292 km (Figure 2 l).

[20] Vertical profiles of residual flows are obviously impacted by stratification (Figure 5). In the upper layer above the halocline, residual currents are highly sheared and intensified. The longitudinal patterns of $\overline{u_R}$ and $\overline{u_D}$ are similar to those of the weakly stratified and partially mixed estuaries. Component $\overline{u_N}$ becomes a two-layer structure with landward flow near the surface. It is remarkable to observe that the two-layer structure of $\overline{u_N}$ is similar to the analytical results given by *Ianniello* [1977] in the case of weak turbulent mixing, despite the fact that the two studies address different systems. Component $\overline{u_A}$ has the typical two-layer structure in the outer regime of the estuary and shows a three-layer structure in the central and inner regimes. The landward flow near the surface is much stronger than that of the partially mixed estuary. Near the head of the estuary (x = 240–250 km), $\overline{u_A}$ is a two-layer structure with landward flow near the surface and seaward flow near the bottom, indicating a reversed asymmetric tidal mixing.

[21] The longitudinal patterns of $\overline{u_R}$ and $\overline{u_D}$ exhibit relatively and qualitatively consistent patterns in the three types of estuaries. Stratification mainly enhances the shear near the surface of the two residual flows. The pattern of ATM-induced flow maintains the typical two-layer structure in the outer regime (near the mouth) of the three types of estuaries, but it changes dramatically in the central

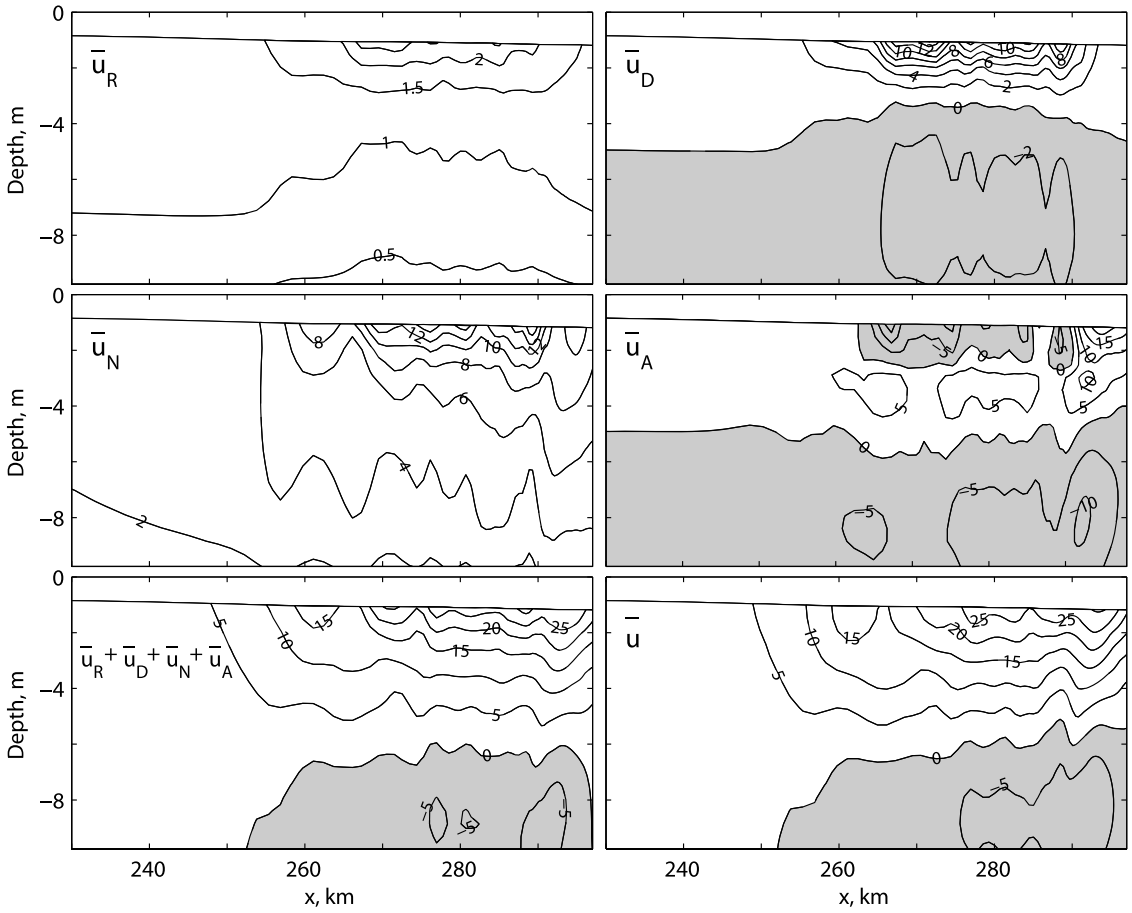

Figure 4. Along-estuary patterns of river-induced ($\overline{u_R}$), density-driven ($\overline{u_D}$), nonlinearities-induced ($\overline{u_N}$), ATM-induced ($\overline{u_A}$), and total Eulerian ($\overline{u}$) residual flows for the partially mixed estuary. The first four residual flows are calculated using the decomposition method (e.g., equations (A1)–(A8)) while the total residual flow is obtained by tidally averaging the modeled current velocity. The units of the residual flow are cm s^{-1}. Negative values (shaded) denote landward flow.

regime as stratification increases. Generally ATM-induced flow reinforces estuarine exchange flow in weakly stratified estuaries, and compensates part of estuarine exchange flow in partially mixed and highly stratified estuaries. The tide-induced flows (both $\overline{u_N}$ and $\overline{u_A}$) impact the entire estuary so that they are important contributors to residual estuarine circulation.

4. Discussion

4.1. Asymmetries in Tidal Mixing

[22] Asymmetries in tidal mixing represent the imbalance of turbulent mixing between flood and ebb tides. Some of previous idealized studies used phasing of stratification in a tidal cycle to measure the asymmetry in tidal mixing [*Stacey et al.*, 2008; *Cheng et al.*, 2010]. This approach splits a tidal cycle into two equal half cycles and presumes that turbulent mixing is stronger in one half cycle than the other. In reality, ATM has a more complicated evolution during a tidal cycle. In order to provide a general measurement of ATM, the depth-mean eddy viscosity ($\langle K_m \rangle$) is integrated over a tidal cycle. Eddy viscosities in flood are represented with positive values while eddy viscosities in ebb are represented by negative values. The sign of the eddy viscosity is taken from the depth-mean current velocity ($\langle u \rangle$):

$$K_{ma} = \frac{1}{T}\int_0^T -sign(\langle u \rangle)\langle K_m \rangle dt, \tag{8}$$

where T is the tidal period, the brackets denote depth-averaged quantities, for example, $\langle u \rangle = (1/D)\int_{-H}^{\eta} u dz$, where $D = \eta + H$, the minus sign appears before $\langle u \rangle$ because u is negative during flood tides in this study. The physical meaning of K_{ma} can be regarded as an excess of tidal mixing over a tidal cycle. Large values of K_{ma} indicate strong tidal asymmetries. Positive ATM (positive values of K_{ma}) represents stronger turbulent mixing during flood tides, while negative ATM (negative values of K_{ma}) represents stronger turbulent mixing during ebb tides. If K_{ma} is zero, there would be no ATM. It is noteworthy that barotropic tidal asymmetry caused by other nonlinear processes can also produce nonzero values of K_{ma}. Therefore, this definition (equation (8)) of K_{ma} is restricted to stratified water columns only.

[23] Asymmetries in tidal mixing were computed for the three types of estuaries (Figure 6). The magnitude of K_{ma} is

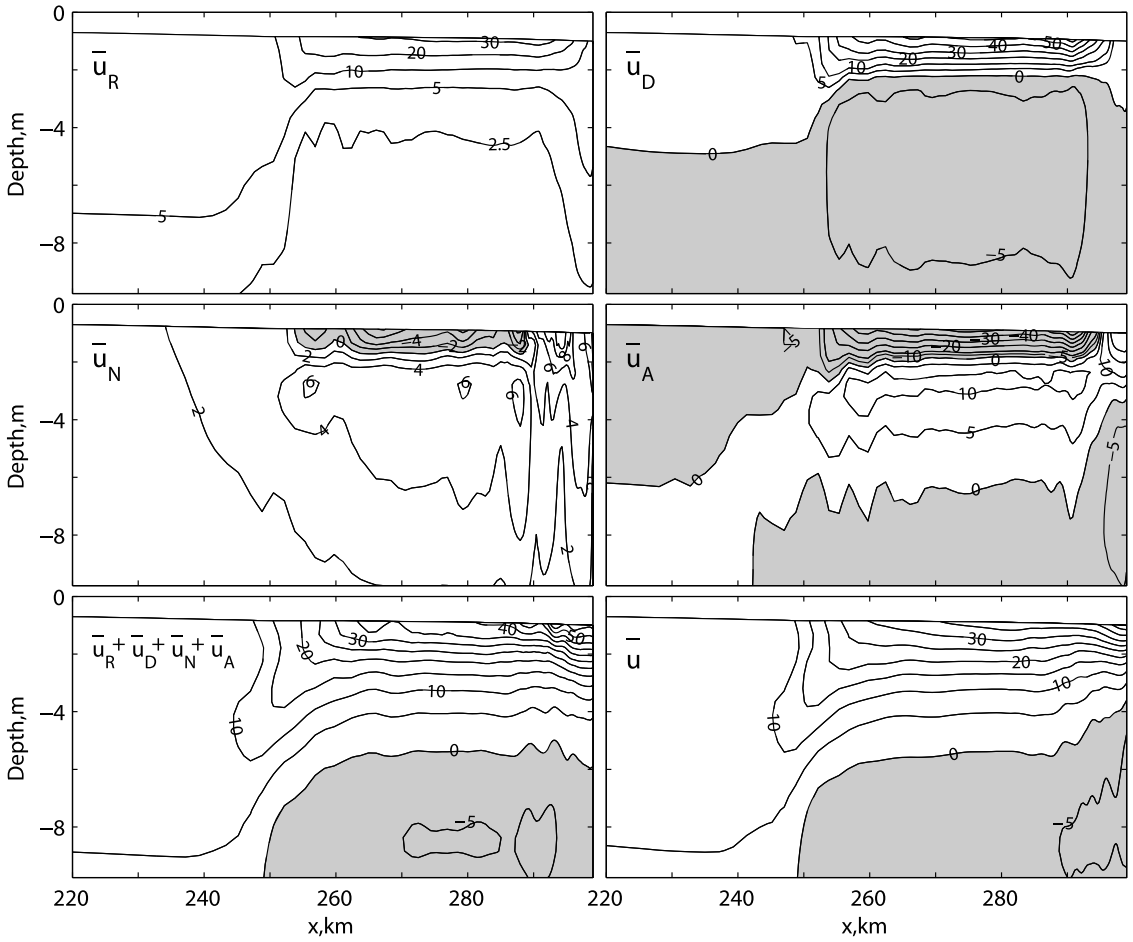

Figure 5. Along-estuary patterns of river-induced ($\overline{u_R}$), density-driven ($\overline{u_D}$), nonlinearities-induced ($\overline{u_N}$), ATM-induced ($\overline{u_A}$), and total Eulerian ($\overline{u}$) residual flows for the highly stratified estuary. The first four residual flows are calculated using the decomposition method (e.g., equations (A1)–(A8)) while the total residual flow is obtained by tidally averaging the modeled current velocity. The units of the residual flow are cm s^{-1}. Negative values (shaded) denote landward flow.

largest in the weakly stratified estuary and smallest in the highly stratified estuary, indicating that stronger tides produce larger ATM. The value of K_{ma} is positive in the estuarine region and is negative in the river region, showing that positive ATM dominates the three types of estuaries. In the highly stratified estuary, K_{ma} is dramatically reduced and becomes negative around the head of the salt intrusion (x = 240–250 km) (Figure 6c). This type of negative ATM has been observed in the upper Chesapeake Bay [*Fugate et al.*, 2007] and has been attributed to advection of stratified waters. During flood tides, stratified water is advected upstream and the water column becomes stratified. During ebb tides, the water column remains well-mixed as depth-uniform freshwater moves downstream. The negative ATM in the river section of the three channels results from the ebb dominant barotropic tides, which may be partially caused by the net seaward freshwater discharge.

4.2. Causes of Vertical Structure of ATM-Induced Flow

[24] The along-estuary distributions of ATM-induced flow in the central regime of estuary change for different types of estuaries. According to equation (A7), the ATM-induced flow is a sum of two contributors. One is driven by the barotropic pressure gradient (the first term on the right hand side of the equation) and the other is driven by the tidally averaged tidal fluctuation component of the vertical shear stress (the "shear force," the second term on the right hand side of the equation). In order to understand the vertical pattern of the ATM-induced flow, it is valuable to examine the spatial structure of the two contributors in the three types of estuaries.

[25] The barotropic pressure gradient

$$\left(g \frac{\partial \overline{\eta_A}}{\partial x} \int_{-H}^{z} \frac{z'}{\overline{K_m}} dz' \right)$$

drives landward currents (negative values) that increase and become amplified near the surface as stratification increases (Figures 7a, 7b, 7c). In contrast, the "shear force"

$$\left(- \int_{-H}^{z} \frac{1}{\overline{K_m}} \overline{K_m' \frac{\partial u'}{\partial z'}} dz' \right)$$

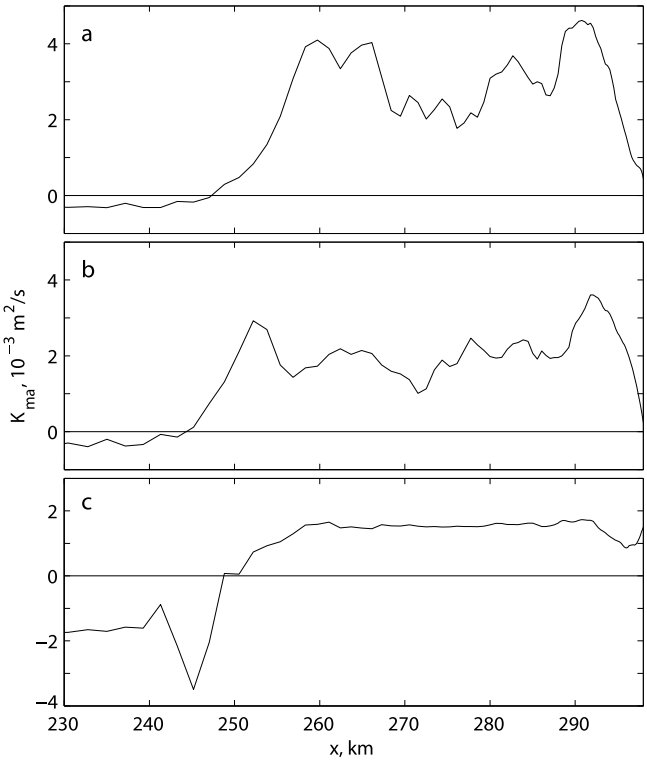

Figure 6. Along-estuary distribution of the asymmetries in tidal mixing (K_{ma}) for (a) the weakly stratified, (b) partially mixed, and (c) highly stratified estuaries.

drives seaward flows that tend to decrease and concentrate near the surface as stratification increases (Figures 7d, 7e, 7f). It is notable that the sea surface of ATM-induced flow is higher at the estuary mouth than at the estuary head. This is opposite to the sea surface slope of density-driven flow. In the weakly stratified estuary, compared to the landward flow (Figure 7a), the seaward flow (Figure 7d) is stronger in the upper layer and is weaker in the lower layer, resulting a two-layer structure. In the partially mixed and highly stratified estuaries, the landward flow is larger than the seaward flow near the surface and bottom, creating a three-layer structure. Particularly, the landward surface flow tends to deepen when stratification becomes stronger.

[26] The "shear force" acts as the driving force of ATM-induced flow so that it partially determines the vertical pattern of ATM-induced flow. Figures 7g, 7h, and 7i shows the along-estuary distribution of $-\overline{k_m' \partial u'/\partial z}$ that is approximately positive in the three types of estuaries. Positive values of $-\overline{k_m' \partial u'/\partial z}$ drive seaward currents (equation (A7)) like those shown in Figures 7d, 7e, and 7f. The magnitude of $-\overline{k_m' \partial u'/\partial z}$ decreases as stratification increases indicating that ATM becomes weaker from weakly to highly stratified estuaries. This is consistent with the along-estuary distribution of K_{ma} (Figure 6). However, the along-estuary patterns of the seaward flows driven by the "shear force" cannot be directly inferred from the distribution of $-\overline{k_m' \partial u'/\partial z}$ because of the influence of tidally averaged vertical eddy viscosity, $\overline{K_m}$ (see equation (A7)). The contribution of $\overline{K_m}$ in determining the vertical distribution of ATM-induced flow will be addressed in section 4.3. The baroclinic pressure gradient has been known as a force driving landward residual estuarine flow. The along-estuary distribution of $-\frac{g}{\rho_0}\int_z^0 \int_{z'}^0 \frac{\partial \rho}{\partial x} dz'' dz'$ (see equation (A3)) is shown in Figures 7j, 7k, and 7l to further examine the role of $-\overline{k_m' \partial u'/\partial z}$ on residual estuarine circulation. In contrast to $-\overline{k_m' \partial u'/\partial z}$,

$$-\frac{g}{\rho_0}\int_z^0 \int_{z'}^0 \frac{\partial \rho}{\partial x} dz'' dz'$$

is negative in the three types of estuaries, suggesting that it acts in an opposite way as $-\overline{k_m' \partial u'/\partial z}$ in driving residual estuarine currents. Also, the opposite sign of the baroclinic pressure gradient and the "shear force" results in sea surface slopes of density-driven and ATM-induced flows that are of opposite sign.

4.3. Turbulent Mixing in the Central Regime of Estuary

[27] The assumption of constant mixing in classical estuarine studies implies that the tidally averaged eddy viscosity is constant in both along-channel and vertical directions. Numerical results have shown that the tidally and vertically averaged eddy viscosity is approximately constant throughout the central regime of the three types of estuaries (Figures 2j, 2k, and 2l), suggesting that constant turbulent mixing could be a valid assumption in that regime of estuary. *Cheng et al.* [2010] attributed this distribution of eddy viscosity in weakly stratified estuaries to the influence of stratification. In this study, we further examine the impact of stratification on turbulent mixing in partially mixed and highly stratified estuaries using the eddy viscosity scale of *Ralston et al.* [2008]:

$$\overline{\langle K_m \rangle} = \frac{a_0 C_d^{3/2} U_T^2 R_{fc}^{1/2}}{g^{1/2} \beta^{1/2} \left(\partial s/\partial x\right)^{1/2}}. \quad (9)$$

Here, a_0 is a constant parameter, β is the haline contraction coefficient (7.7×10^{-4}), C_d is the bottom drag coefficient, s is salinity, U_T is the tidal current amplitude, R_{fc} is the critical flux Richardson number (chosen 0.2 here). In this scaling, the along-channel salinity gradient accounts for the influence of stratification. The predicted eddy viscosities are approximately constant in the central regime of the estuary and generally agree with those modeled (Figures 2j, 2k, and 2l). In particular, the highly stratified estuary has the best agreement, suggesting that this scaling for the eddy viscosity is even more reliable in stratified estuaries. The parameter a_0 is obtained by best fitting the modeled eddy viscosities. The values of a_0 for the three types of estuaries are 0.31, 0.32 and 0.34, respectively, increasing as stratification increases. Therefore, the parameter a_0 is also a function of stratification and the scaling of the eddy viscosity needs further study.

[28] Stratification modifies the vertical structure of the eddy viscosity, which usually is assumed to have a parabolic shape in a homogeneous open channel flow. The vertical profiles of tidally averaged eddy viscosities in the central regime of the three estuaries exhibit an asymmetric shape, with greatest values found in the lower half of the water

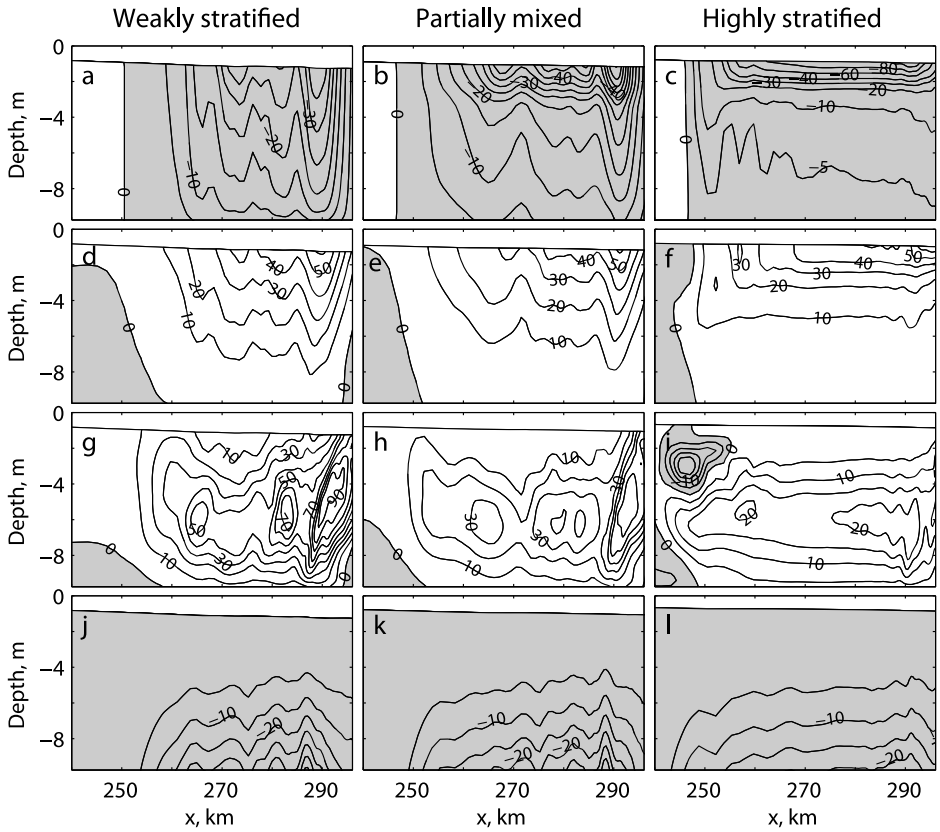

Figure 7. (a-c) Along-estuary distributions of the barotropic pressure gradient of ATM-induced flow; (d-f) the "shear forcing" of ATM-induced flow; (g-i) tidally averaged shear stress variation; and (j-l) baroclinic pressure gradient. The units of Figures 7a–7f are cm/s, and the units of Figures 7g–7l are 10^{-5} m^2/s^2. Negative values are shaded.

column (Figure 8). As stratification increases, the maximum value of eddy viscosity shifts toward the bottom and the eddy viscosities near the surface become small. The vertical distribution of eddy viscosity affects the vertical patterns of residual currents. In the analytical model of *Cheng et al.* [2010], the tidal mean eddy viscosity is assumed constant, resulting in a two-layer flow structure of ATM-induced flow with almost equal thickness for each layer. In the weakly stratified estuary, a constant eddy viscosity would predict relatively reasonable vertical profiles of ATM-induced flow (Figure 3). However, as stratification increases, the vertical distribution of ATM-induced flow by varying eddy viscosity gradually deviates from that predicted by the analytical solution and tends to a three-layer structure. Consequently, appropriate vertical profiles of eddy viscosity as shown in Figure 8 are required to determine ATM-induced flow under strong stratification. According to the solution of ATM-induced flow (e.g., equation (A7)), the small eddy viscosities in the upper water column lead to amplified currents, resulting in landward residual flow near the surface under strong stratification. This explains the evolution of the two components of ATM-induced flow along with increasing stratification (Figures 7a–7f).

[29] The vertical distribution of tidal mean eddy viscosity also affects the river-induced, the density-driven and the nonlinearities-induced flows (equations (A1)–(A6)). With greater stratification, these flows tend to increase and concentrate near the surface because of the small eddy viscosity in the upper water column (Figures 3–5). The classical theory of estuarine gravitational circulation assumed that the tidally averaged eddy viscosity is vertically constant, and showed the thickness of the two layers of current velocity is not related to eddy viscosity [e.g., *Hansen and Rattray*, 1966]. This study, however, demonstrates that an appropriate vertical distribution of tidal mean eddy viscosity is crucial to describe the vertical structure of estuarine gravitational circulation under strong stratification.

4.4. Strength of ATM-Induced Residual Flow

[30] Because some components of the residual flows are not unidirectional, the intensity of currents is used to measure the strength of residual flows instead of the depth-mean following *Burchard and Hetland* [2010]:

$$\langle|\overline{u}|\rangle = \frac{1}{H}\int_{-H}^{0}|\overline{u}|dz, \tag{10}$$

where $|\overline{u}|$ is the absolute value of the residual current velocity. The strength of the ATM-induced flows is compared to that of the density-driven flows to determine their relative contribution to estuarine exchange flow. The other two components (nonlinearities-induced and river-driven flows) and the total residual flow are omitted.

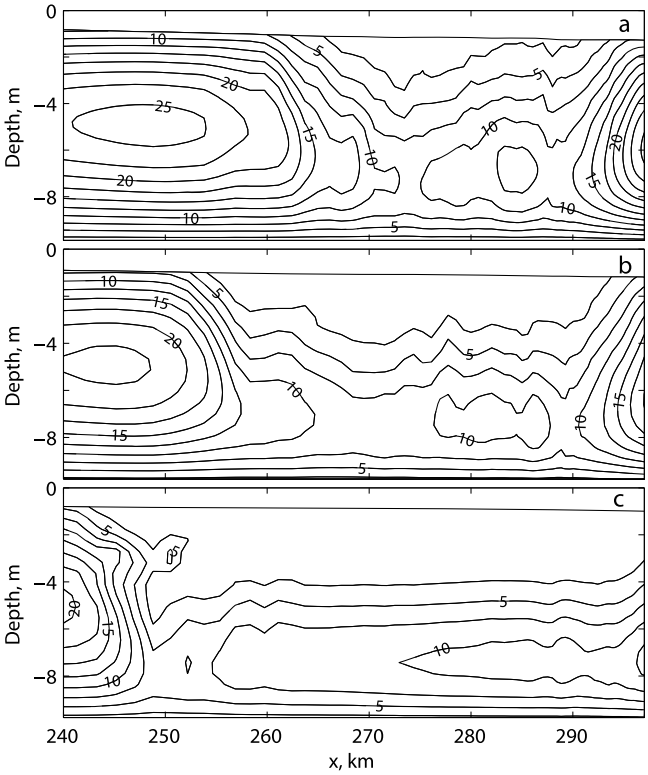

Figure 8. Contour plots of tidally averaged eddy viscosity for (a) the weakly stratified, (b) partially mixed, (c) and highly stratified estuaries. The units are $\times 10^{-3}$ m^2 s^{-1}.

[31] In the central regime of the estuary, the strength of the ATM-induced flow is much larger than that of the density-driven flow in weakly stratified estuaries. It is approximately twice in partially mixed estuaries, and it is smaller in highly stratified estuaries (Figure 9). This relationship shows that the relative contribution of ATM-induced flow to residual estuarine circulation decreases as stratification increases. The strength of density-driven flow rapidly increases as stratification becomes stronger, in accordance with the classical theory of estuarine gravitational circulation. The strength of ATM-induced flow, in contrast, varies insignificantly in the three types of estuaries. The along-estuary distributions of the intensity of ATM-induced flow are different in the central regime of estuary under the influence of stratification. In weakly stratified and partially mixed estuaries, the amplitude of ATM-induced flow decreases from near the mouth toward the head, while in the highly stratified estuary, the intensity of ATM-induced flow is approximately constant.

[32] According to the solution of ATM-induced flow (equation (A7)), the magnitude of depth-averaged ATM-induced residual flow can be parameterized as a function of tidal current amplitude (U_T), asymmetries in tidal mixing (K_{ma}), and tidally and vertically averaged eddy viscosity:

$$|\langle \overline{u_A} \rangle| = \frac{K_{ma}}{\langle \overline{K_m} \rangle} U_T \frac{H}{\sqrt{2\langle \overline{K_m} \rangle/\omega}}, \tag{11}$$

where ω is the angular frequency of tidal forcing. The term $\sqrt{2\langle \overline{K_m} \rangle/\omega}$ represents the thickness of the Stokes boundary layer, in which velocity shear is significant. Here, we choose U_T and K_{ma} to represent tidal fluctuation component of vertical shear stress. We further write equation (11) to

$$|\langle \overline{u_A} \rangle| = c_0 K_{ma}^{c_1} U_T^{c_2} \overline{\langle K_m \rangle}^{c_3}, \tag{12}$$

where c_0, c_1, c_2 and c_3 are parameters determined by least square fitting numerical results in the central and inner regimes of the estuaries (Table 1). The fitted coefficient c_3 is approximately -1.0 for the three estuaries in accordance with equation (A7). Coefficient c_1 is much smaller than coefficient c_2 in the weakly stratified estuary and is larger than coefficient c_2 in the highly stratified estuary. This demonstrates that the strength of ATM-induced flow is highly related to tidal current amplitude in the weakly stratified estuary and is mainly regulated by asymmetries in tidal mixing in the highly stratified estuary. These dependences are consistent with the along-estuary distributions of the asymmetries in tidal mixing and of the tidal current amplitude, both of which decrease toward the estuary head (Figure 6).

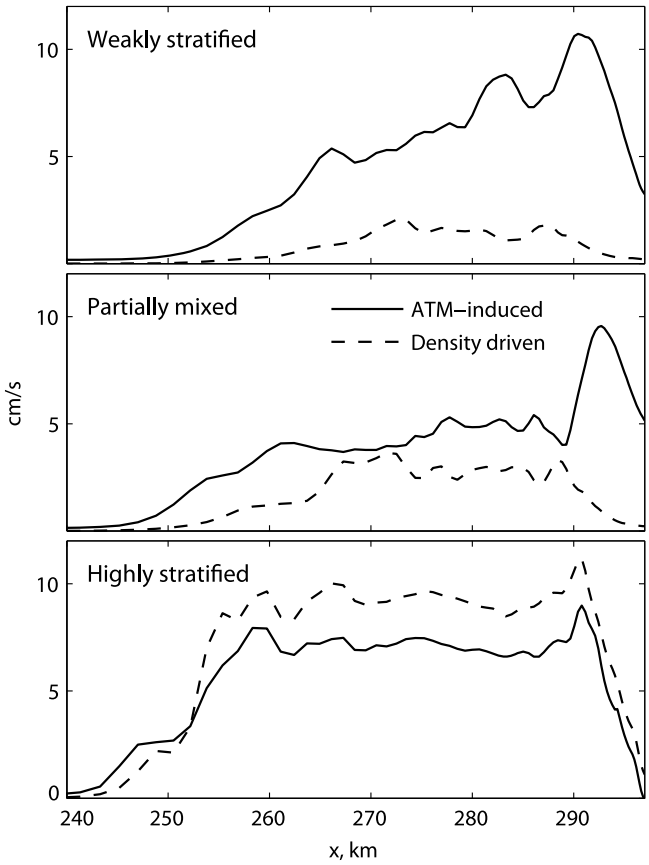

Figure 9. Along-estuary distributions of the intensities of ATM-induced and density-driven flows in (top) the weakly stratified, (middle) partially mixed, and (bottom) highly stratified estuaries. The units of the residual flows are cm s^{-1}.

Table 1. Least Squares Fit of the Strength of Asymmetric Tidal Mixing-Induced Flow

	c_0 ($\times 10^{-3}$)	c_1	c_2	c_3	r^2
Weakly stratified	0.003	0.46	4.32	−1.15	0.91
Partially mixed	0.13	1.02	1.15	−0.76	0.81
Highly stratified	0.02	1.16	0.34	−0.97	0.79

[33] The fitting of equation (12) has relatively high correlation coefficients (r^2) showing that the magnitude of ATM-induced flow can be estimated using equation (12). However, the fitted parameters change for different types of estuaries and might be functions of stratification. The general scale of ATM-induced flow is still to be explored.

5. Summary and Conclusions

[34] The asymmetry in turbulent mixing between flood and ebb tides contributes to the creation of residual estuarine currents. To address residual currents induced by asymmetric tidal mixing in estuaries, it is essential to extract ATM-induced flows from total residual currents. This study provides a method to decompose residual estuarine currents into four components: river-induced, density-driven, nonlinearities-induced and ATM-induced flows. This method works well with numerical model results, and has the potential to be applied to field data if detailed information on vertical eddy viscosities and tidal current velocities are available.

[35] The decomposition of residual estuarine currents into four contributions allows illustration of the along-estuary distribution of ATM-induced flow in three types of coastal plain estuaries: weakly stratified, partially mixed and highly stratified, on the basis of a series of idealized numerical experiments. The along-estuary patterns of the ATM-induced flow in the estuarine central regime are influenced by stratification. In weakly stratified estuaries, the ATM-induced flow has a two-layer structure similar to that of density-driven flow. It reinforces the estuarine exchange flow. In partially mixed and highly stratified estuaries, the ATM-induced flow tends to have a three-layer structure with landward flows near the surface and bottom, and seaward flow in the middle of the water column. The vertical distribution of the ATM-induced flow is determined by the tidally averaged shear stress variation and vertical eddy viscosity, which are both highly influenced by stratification.

[36] The relative importance of ATM-induced flow to residual estuarine currents is evaluated by the comparison of density-driven flow. ATM-induced flows dominate density-driven flows in weakly stratified estuaries, are similarly important in partially mixed estuaries, and are less important in highly stratified estuaries. The strength of the ATM-induced flow can be related to tidal current amplitude, asymmetries in tidal mixing and the tidal mean vertical eddy viscosity.

Appendix A: Solutions of Residual Flows

[37] Equations (4a)–(5b) can be solved by vertically integrating the momentum equations and applying continuity and boundary conditions. The solution for river-induced flow is

$$\overline{u_R} = g\frac{\partial \overline{\eta_R}}{\partial x}\int_{-H}^{z}\frac{z'}{\overline{K_m}}dz', \tag{A1}$$

$$\frac{\partial \overline{\eta_R}}{\partial x} = \frac{R}{g\int_{-H}^{0}\int_{-H}^{z}\frac{z'}{\overline{K_m}}dz'dz}. \tag{A2}$$

The solution for density-driven flow is

$$\overline{u_D} = g\frac{\partial \overline{\eta_D}}{\partial x}\int_{-H}^{z}\frac{z'}{\overline{K_m}}dz' - \frac{g}{\rho_0}\int_{-H}^{z}\left(\frac{1}{\overline{K_m}}\int_{z'}^{0}\int_{z''}^{0}\frac{\partial \overline{\rho}}{\partial x}dz'''dz''\right)dz', \tag{A3}$$

$$\frac{\partial \overline{\eta_D}}{\partial x} = \frac{1}{\rho_0}\frac{\int_{-H}^{0}\int_{-H}^{z}\left(\frac{1}{\overline{K_m}}\int_{z'}^{0}\int_{z''}^{0}\frac{\partial \overline{\rho}}{\partial x}dz'''dz''\right)dz'dz}{\int_{-H}^{0}\int_{-H}^{z}\frac{z'}{\overline{K_m}}dz'dz}. \tag{A4}$$

The solution for nonlinearities-induced residual flow is

$$\overline{u_N} = g\frac{\partial \overline{\eta_N}}{\partial x}\int_{-H}^{z}\frac{z'}{\overline{K_m}}dz' - \int_{-H}^{z}\left(\frac{1}{\overline{K_m}}\int_{z'}^{0}\left(\overline{u\frac{\partial u}{\partial x}} + \overline{w\frac{\partial u}{\partial z''}}\right)dz''\right)dz', \tag{A5}$$

$$\frac{\partial \overline{\eta_N}}{\partial x} = \frac{\int_{-H}^{0}\int_{-H}^{z}\left(\frac{1}{\overline{K_m}}\int_{z'}^{0}\left(\overline{u\frac{\partial u}{\partial x}} + \overline{w\frac{\partial u}{\partial z''}}\right)dz''\right)dz'dz - \overline{u|_{z=0}\eta}}{g\int_{-H}^{0}\int_{-H}^{z}\frac{z'}{\overline{K_m}}dz'dz}. \tag{A6}$$

The solution for ATM-induced residual flow is

$$\overline{u_A} = g\frac{\partial \overline{\eta_A}}{\partial x}\int_{-H}^{z}\frac{z'}{\overline{K_m}}dz' - \int_{-H}^{z}\frac{1}{\overline{K_m}}\overline{K_m'\frac{\partial u'}{\partial z'}}dz', \tag{A7}$$

$$\frac{\partial \overline{\eta_A}}{\partial x} = \frac{\int_{-H}^{0}\int_{-H}^{z}\frac{1}{\overline{K_m}}\overline{K_m'\frac{\partial u'}{\partial z'}}dz'dz}{g\int_{-H}^{0}\int_{-H}^{z}\frac{z'}{\overline{K_m}}dz'dz}, \tag{A8}$$

where z', z'', and z''' are dummy variables. The vertical eddy viscosity is depth dependent instead of constant. The solution to the ATM-induced flow is determined from the tidal variation of vertical shear stress divergence. This is consistent with the mathematical definition given by *Burchard and Hetland* [2010]. The solution for the density-driven flow is similar to that given by *Officer* [1976] because

both solutions are based on a linear longitudinal momentum balance.

[38] **Acknowledgments.** This work was supported by NSF Project OCE-0726697. We thank two anonymous reviewers for their insightful comments that helped improve this work.

References

Burchard, H., and R. D. Hetland (2010), Quantifying the contributions of tidal straining and gravitational circulation to residual circulation in periodically stratified tidal estuaries, *J. Phys. Oceanogr.*, *40*(6), 1243–1262, doi:10.1175/2010JPO4270.1.

Cameron, W. M., and D. W. Pritchard (1963), Estuaries, in *The Sea*, vol. 2, edited by M. N. Hill, pp. 306–324, John Wiley, New York.

Chatwin, P. C. (1976), Some remarks on the maintenance of the salinity distribution in estuaries, *Estuarine Coastal Mar. Sci.*, *4*, 555–566, doi:10.1016/0302-3524(76)90030-X.

Cheng, P., and A. Valle-Levinson (2009), Influence of lateral advection on residual currents in microtidal estuaries, *J. Phys. Oceanogr.*, *39*(12), 3177–3190, doi:10.1175/2009JPO4252.1.

Cheng, P., A. Valle-Levinson, and H. E. de Swart (2010), Residual currents induced by asymmetric tidal mixing in weakly stratified narrow estuaries, *J. Phys. Oceanogr.*, *40*(9), 2135–2147, doi:10.1175/2010JPO4314.1.

Fram, J. P., M. Martin, and M. T. Stacey (2007), Exchange between the coastal ocean and a semi-enclosed estuarine basin: Dispersive fluxes, *J. Phys. Oceanogr.*, *37*, 1645–1660, doi:10.1175/JPO3078.1.

Fugate, D. C., C. T. Friedrichs, and L. P. Sanford (2007), Lateral dynamics and associated transport of sediment in the upper reaches of a partially mixed estuary, Chesapeake Bay, USA, *Cont. Shelf Res.*, *27*, 679–698, doi:10.1016/j.csr.2006.11.012.

Haidvogel, D. B., H. G. Arango, K. Hedstrom, A. Beckmann, P. Malanotte-Rizzoli, and A. F. Shchepetkin (2000), Model evaluation experiments in the North Atlantic Basin: Simulations in nonlinear terrain-following coordinates, *Dyn. Atmos. Oceans*, *32*, 239–281, doi:10.1016/S0377-0265(00)00049-X.

Hansen, D. V., and M. Rattray (1966), Gravitational circulation in straits and estuaries, *J. Mar. Res.*, *23*, 104–122.

Huijts, K. M. H., H. M. Schuttelaars, H. E. de Swart, and C. T. Friedrichs (2009), Analytical study of the transverse distribution of along-channel and transverse residual flows in tidal estuaries, *Cont. Shelf Res.*, *29*, 89–100, doi:10.1016/j.csr.2007.09.007.

Ianniello, J. P. (1977), Tidally induced residual currents in estuaries of constant breadth and depth, *J. Mar. Res.*, *35*, 755–786.

Ianniello, J. P. (1981), Comments on tidally induced residual currents in estuaries: Dynamics and near bottom flow characteristics, *J. Phys. Oceanogr.*, *11*, 126–134, doi:10.1175/1520-0485(1981)011<0126:COTIRC>2.0.CO;2.

Jay, D. A., and J. M. Musiak (1996), Internal tidal asymmetry in channel flows: Origins and consequences, in *Mixing Processes in Estuaries and Coastal Seas*, *Coastal Estuarine Stud. Ser.*, vol. 50, edited by C. Pattiaratchi, pp. 211–249, AGU, Washington, D. C.

Jay, D. A., and J. D. Smith (1990), Residual circulation in shallow estuaries: 2. Weakly stratified and partially mixed, narrow estuaries, *J. Geophys. Res.*, *95*, 733–748, doi:10.1029/JC095iC01p00733.

Lacy, J. R., M. T. Stacey, J. R. Burau, and S. G. Monismith (2003), The interaction of lateral baroclinic forcing and turbulence in an estuary, *J. Geophys. Res.*, *108*(C3), 3089, doi:10.1029/2002JC001392.

Lerczak, J. A., and W. R. Geyer (2004), Modeling the lateral circulation in straight, stratified estuaries, *J. Phys. Oceanogr.*, *34*, 1410–1428, doi:10.1175/1520-0485(2004)034<1410:MTLCIS>2.0.CO;2.

MacCready, P. (2004), Toward a unified theory of tidally averaged estuarine salinity structure, *Estuaries*, *27*(4), 561–570, doi:10.1007/BF02907644.

McCarthy, R. K. (1993), Residual currents in tidally dominated, well-mixed estuaries, *Tellus, Ser. A*, *45*, 325–340.

Officer, C. B. (1976), *Physical Oceanography of Estuaries (and Associated Coastal Waters)*, John Wiley, New York.

Pritchard, D. W. (1952), Salinity distribution and circulation in the Chesapeake Bay estuarine system, *J. Mar. Res.*, *11*(2), 106–123.

Pritchard, D. W. (1955), Estuarine circulation patterns, *Proc. Am. Soc. Civ. Eng.*, *81*(717), 1–11.

Pritchard, D. W. (1956), The dynamic structure of a coastal plain estuary, *J. Mar. Res.*, *15*(1), 33–42.

Ralston, D. K., W. R. Geyer, and J. A. Lerczak (2008), Subtidal salinity and velocity in the Hudson River estuary: Observations and modeling, *J. Phys. Oceanogr.*, *38*, 753–770, doi:10.1175/2007JPO3808.1.

Scully, M. E., W. R. Geyer, and J. A. Lerczak (2009), The influence of lateral advection on the residual estuarine circulation: A numerical modeling study of the Hudson River estuary, *J. Phys. Oceanogr.*, *39*, 107–124, doi:10.1175/2008JPO3952.1.

Simpson, J. H., J. Brown, J. Matthews, and G. Allen (1990), Tidal straining, density currents, and stirring in the control of estuarine stratification, *Estuaries*, *13*(2), 125–132, doi:10.2307/1351581.

Stacey, M. T., J. R. Burau, and S. G. Monismith (2001), Creation of residual flows in a partially stratified estuary, *J. Geophys. Res.*, *106*, 17,013–17,037, doi:10.1029/2000JC000576.

Stacey, M. T., J. P. Fram, and F. K. Chow (2008), Role of tidally periodic density stratification in the creation of estuarine subtidal circulation, *J. Geophys. Res.*, *113*, C08016, doi:10.1029/2007JC004581.

Talke, S. A., H. E. de Swart, and H. M. Schuttelaars (2009), Feedback between residual circulations and sediment distribution in highly turbid estuaries: An analytical model, *Cont. Shelf Res.*, *29*(1), 119–135, doi:10.1016/j.csr.2007.09.002.

P. Cheng, Large Lakes Observatory, University of Minnesota, Duluth, MN 55812, USA. (chengp@d.umn.edu)

H. E. de Swart, Institute for Marine and Atmospheric Research Utrecht, Utrecht University, Princetonplein 5, NL-3584 CC Utrecht, Netherlands.

A. Valle-Levinson, Department of Civil and Coastal Engineering, University of Florida, Gainesville, FL 32611, USA.